Inverse Synthetic Aperture Radar Imaging Via Modified Smoothed L_0 Norm

Jieqin Lv, Lei Huang, *Member, IEEE*, Yunmei Shi, and Xiongjun Fu

***Abstract*—Compressive sensing theory is able to exactly recover an unknown sparse signal from observation samples with high probability. In this letter, we convert the imaging into a problem of signal reconstruction with the aid of orthogonal basis in the framework of high-resolution inverse synthetic aperture radar imaging. More specifically, we propose a new method based on smoothed L_0 norm, whose recovery rate is faster than the algorithm based on L_1 norm. Experiment results with real data show that our proposal is more efficient than the L_1 norm algorithm.**

***Index Terms*—Compressive sensing, inverse synthetic aperture radar, signal reconstruction, smoothed L_0 norm.**

I. Introduction

As A powerful signal processing technique, inverse synthetic aperture radar (ISAR) is able to image moving targets in range and cross-range domains. Basically, ISAR processing is used for target identification and classification. Due to its wide application, high-resolution ISAR imaging has received much attention in the literature, such as [1]–[4]. In order to obtain high resolution, we need to increase the transmitted signal bandwidth and coherent processing interval (CPI). The former determines the range resolution, which is limited by the radar system, whereas the latter determines the cross-range resolution. However, large CPI can lead to some problems: 1) It can make the target-motion compensation more complex. 2) Because of the uncooperative character of the targets, large observing interval for data collection may be unachievable. As a result, how to obtain enough measured data is the key problem. Some methods such as MUSIC [5] can achieve super-resolution profile, but require more accurate estimations of the covariance matrix and model orders. Under the conditions that the radar data sampling rate is small and observation data are lost partially, these methods cannot provide good profile. Compressive sensing (CS) is a signal processing technique for efficiently acquiring and reconstructing a signal by finding solutions to underdetermined linear systems. The CS theory takes advantage of the sparseness or compressibility of signals in some domain, allowing the entire signal to be determined from relatively few measurements. The key issue of CS is to find the sparse solution of the underdetermined linear systems. When the dimension increases, it is shown in [6] that solving the minimum L_0 norm is an intractable problem. Moreover, it is sensitive to noise. Some authors have proposed successful approaches such as Basis Pursuit (BP) [7] and L_1-SVD [8], which finds the sparse solution by minimizing the L_1 norm. The methods based on minimum L_1 norm need a large system of equations. In [9], it is revealed that the algorithms based on smoothed L_0 norm (SL_0) can achieve the same (or higher) accuracy under small sample scenarios and has the faster convergence rate.

Manuscript received May 12, 2014; accepted June 17, 2014. Date of publication June 30, 2014; date of current version July 08, 2014. The work described in this letter was supported in part by a grant from the NSFC/RGC Joint Research Scheme sponsored by the Research Grants Council of Hong Kong and the National Natural Science Foundation of China (Project No.: N_CityU 104/11, 61110229/61161160564), the National Natural Science Foundation of China under Grants 61222106 and 61171187, and the Shenzhen Kongqie talent program under Grant KQC201109020061A.

J. Lv, L. Huang, and Y. Shi are with the Department of Electronic and Information Engineering, Harbin Institute of Technology Shenzhen Graduate School, Shenzhen 518055, China (e-mail: dr.lei.huang@ieee.org).

X. Fu is with the Department of Electronic Engineering, Beijing Institute of Technology, Beijing 100081, China.

Color versions of one or more of the figures in this letter are available online at http://ieeexplore.ieee.org.

Digital Object Identifier 10.1109/LAWP.2014.2332639

In this letter, we address the radar high-resolution imaging model and transform it into a sparse signal representation problem. Based on the smoothed L_0 norm method, we propose a modified smoothed L_0 norm (MSL_0) method that can give a better sparse solution. The experimental results show that the proposed approach can obtain high-quality image under the scenarios where the data sampling rate is small and data are lost partially.

II. ISAR Model and Imaging

Assume the radar signals are on the conditions of free space propagation and far-field plane wave approximation. The backscattered characteristics are described by an ideal point-scattering model. Suppose that the radar transmits a linear frequency-modulated signal and the radar echo from a point is

$$z(\tau,t)=x\cdot \mathrm{U}\left(\frac{\tau-\gamma}{T_{\mathrm{p}}}\right)\cdot e^{j2\pi\left(f_{\mathrm{c}}(\tau-\gamma)+\frac{\kappa}{2}(\tau-\gamma)^2\right)}\mathrm{U}\left(\frac{t}{T_{\mathrm{a}}}\right) \quad (1)$$

where κ and f_{c} are the chirp rate and carrier frequency, respectively, T_{a} is the observed duration, T_{p} is the pulse duration of single pulse, τ is the fast time, t is the slow time, x is the scattering amplitude, and $\mathrm{U}(\tau/T_{\mathrm{p}})$ is the unit rectangular function. We have converted the range variable $r(t)$ into time delay $\gamma=2r(t)/c$, where c is the propagation velocity of light.

Assume that the translational motion has been removed by the conventional compensation, the range compression has been conducted, and the phase error has been corrected. Moreover, we assume that the range cell contains N scattering centers with different cross-range locations. If the rotational motion is stationary, we have the complex envelope of the echo signal in the range cell

$$z(t)=\sum_{n=1}^{N}x_n\cdot \mathrm{U}\left(\frac{t}{T_{\mathrm{a}}}\right)\cdot e^{-j2\pi f_n t}. \quad (2)$$

1536-1225 © 2014 IEEE. Personal use is permitted, but republication/redistribution requires IEEE permission.
See http://www.ieee.org/publications_standards/publications/rights/index.html for more information.

After cross-range compression by applying azimuth Fourier transform to (2), the signal is written as

$$z(f) = \sum_{n=1}^{N} x_n \cdot \mathrm{sinc}\left[T_a(f - f_n)\right] \tag{3}$$

where f represents the Doppler frequency. As the cross-range coordinate of a scattering center is proportional to f_n, the image formation of target can be resolved in the Range-Doppler (RD) domain. This is the RD framework where the cross-range axis is replaced by the Doppler axis. According to the scattering properties of an object, we know that the strong scattering centers have large scattering coefficients and make the main contribution to the image formation. On the contrary, the weak scattering centers and noise have little contribution to the image formation. As a result, the radar echoes are of sparsity. In this letter, we use the sparsity as the global metric of image and construct an imaging algorithm based on the compressive sensing theory.

III. ISAR Imaging via CS

A. CS-Based Imaging Model

In order to recovery signal from limited measurements, some authors have used the theory of CS [10], [11]. Let $\mathbf{y} \in \mathbb{C}^N$ be a signal we wish to decompose over a given basis $\mathbf{B} = [\mathbf{b_1}, \cdots, \mathbf{b_N}]$. We then have $\mathbf{y} = \mathbf{B}\mathbf{x} = \sum_{i=1}^{N} x_i \mathbf{b_i}$, where $\mathbf{x} = [x_1, \cdots, x_n]^T$ is the corresponding coefficient vector. If $\mathbf{x}$ includes K largest coefficients, then we define $\mathbf{x}$ as a K sparse vector [10]. Utilizing the measurement matrix $\mathbf{\Psi}$, we can get $\mathbf{z} = \mathbf{\Psi}\mathbf{y} = \mathbf{\Psi}\mathbf{B}\mathbf{x} = \mathbf{A}\mathbf{x}$, where $\mathbf{A} \in \mathbb{C}^{M\times N}$ $(M < N)$ and $\mathbf{z} \in \mathbb{C}^M$. If the dictionary matrix $\mathbf{A}$ satisfies the restricted isometry property (RIP) [12] and $M > O(K \cdot \log N)$, the coefficients can be recovered from $\mathbf{z}$ with overwhelming probability by solving

$$\min \|\mathbf{x}\|_0 \quad \text{subject to} \quad \mathbf{A}\mathbf{x} = \mathbf{z} \tag{4}$$

where $\|\cdot\|_0$ denotes the L_0 norm, i.e., number of the nonzero components of $\mathbf{x}$. However, (4) is an intractable problem since it requires combinational search, as has been pointed out in [11]. To seek the solution, one resorts to the minimum L_p norm, where p satisfies $0 < p \leq 2$. Unlike the minimum L_p norm method, the smoothed L_0 norm algorithm directly minimizes the L_0 norm by using a continue function to approximate it.

The noisy signal at the range cell model for short CPI can be rewritten as

$$\mathbf{z} = \sum_{n=1}^{N} x_n \cdot \mathrm{U}\left(\frac{\mathbf{t}}{T_\mathrm{a}}\right) \cdot e^{-j2\pi f_n \mathbf{t}} + \mathbf{e} \tag{5}$$

where $\mathbf{e}$ is the synthetic additive noise in the range cell. Assume that f_r is the pulse repetition frequency, $t' = 1/f_\mathrm{r}$ is the time resolution, $Q = T_\mathrm{a}/t'$ is the pulse number, and the time vector is $t = [1 : Q]^T t'$. We also define f'_d is the frequency resolution. As a result, the discrete Doppler vector is $\mathbf{f_d} = [1 : N]^T f'_\mathrm{d}$. Then, we get the sparse basis matrix $\mathbf{B}$ for the radar echo signal

$$\mathbf{B} = \begin{pmatrix} e^{-j2\pi f'_\mathrm{d} t'} & e^{-j2\pi 2 f'_\mathrm{d} t'} & \cdots & e^{-j2\pi N f'_\mathrm{d} t'} \\ e^{-j2\pi f'_\mathrm{d} 2t'} & e^{-j2\pi 2 f'_\mathrm{d} 2t'} & \cdots & e^{-j2\pi N f'_\mathrm{d} 2t'} \\ \vdots & \vdots & & \vdots \\ e^{-j2\pi f'_\mathrm{d} Qt'} & e^{-j2\pi 2 f'_\mathrm{d} Qt'} & \cdots & e^{-j2\pi N f'_\mathrm{d} Qt'} \end{pmatrix}$$

and choose a random partial unit matrix (namely, randomly selected M rows from the unit matrix $\mathbf{I}_{Q\times Q}$) as the measurement matrix

$$\mathbf{\Psi} = \begin{pmatrix} 1 & 0 & 0 & 0 & \cdots & 0 \\ 0 & 0 & 1 & 0 & \cdots & 0 \\ \vdots & \vdots & & \vdots & \vdots & \vdots \\ 0 & 0 & 0 & 0 & \cdots & 1 \end{pmatrix}$$

where $\mathbf{\Psi} \in \mathbb{R}^{M\times Q}$ $(M < Q)$. Thus, we get the dictionary matrix $\mathbf{A} = \mathbf{\Psi} \times \mathbf{B}$. As the Fourier matrix has a better noncoherence than the Gaussian matrix when used as a dictionary matrix, it will be employed in this letter. Obviously, the dictionary matrix $\mathbf{A}$ is the partial Fourier matrix, which satisfies the RIP. Therefore, we can recover the original signal from the measurements via the dictionary matrix. Then, we can convert the radar imaging model to the new imaging model based on CS

$$\mathbf{z} = \mathbf{A}\mathbf{x} + \mathbf{e} \tag{6}$$

where $\mathbf{x}$ represents the amplitudes of the scattering points. Therefore, we can get the amplitudes of the scattering points by solving

$$\min \|\mathbf{x}\|_0, \quad \text{s.t. } \|\mathbf{A}\mathbf{x} - \mathbf{z}\|_2 \leq \epsilon \tag{7}$$

where ϵ is an upper bound for the noise level. As mentioned above, it is difficult to apply the L_0 norm to obtain the solution because the L_0 norm of a vector is highly discontinuous. Thus, we approximate it using a continuous Gaussian function.

B. Modified Smoothed L_0 Norm Approximation

The smoothed L_0 norm approaches are based on the approximate L_0 norm with a sequence of continuous functions. These methods turn out to be the L_0 norm as $\sigma \to 0$ in some sense [9]. As a result, we can use the following function to approximate the L_0 norm:

$$F_\sigma(\mathbf{x}) = \sum_{i=1}^{N} f_\sigma(x_i) \tag{8}$$

which converges to the L_0 norm as $\sigma \to 0$, where

$$f_\sigma(x) \triangleq e^{\left(\frac{-x^2}{2\sigma^2}\right)} \tag{9}$$

and

$$\lim_{\sigma\to 0} f_\sigma(x) = \begin{cases} 1, & \text{if } (x = 0) \\ 0, & \text{if } (x \neq 0). \end{cases} \tag{10}$$

It is clear from (9) that $\|\mathbf{x}\|_0 \approx N - F_\sigma(\mathbf{x})$ for small values of σ. Moreover, when $\sigma \to 0$, this approximation becomes equality. In practical scenarios, the observations are contaminated, and the sampling model is $\mathbf{z} = \mathbf{A}\mathbf{x} + \mathbf{e}$, where $\mathbf{e}$ represents the additive zero-mean white noise. Then, we can obtain the sparse solution by solving

$$\max_{\mathbf{x}} F_\sigma(\mathbf{x}), \quad \text{s.t. } \|\mathbf{Ax}-\mathbf{z}\|_2 \leq \epsilon. \tag{11}$$

It is shown in [9] that for small values of σ, $F_\sigma(\mathbf{x})$ is highly nonsmooth and has several local maxima that lead to the difficulty of its maximization. However, for large values of σ, F_σ is smoother and contains less local maxima so that the maximization procedure can be easily carried out. Therefore, we choose a decreasing sequence for σ and maximize the F_σ for each value of σ. Based on the method of [14], we use the weighted least-squares approach to modify the initial value so that the modified smoothed L_0 norm algorithm can converge to the sparse solution faster and more accurate. For the noisy case, it is noticed that using the Lagrangian function, the problem can be written as

$$\hat{\mathbf{x}} = \arg\min_{\mathbf{x}} \|\mathbf{Ax}-\mathbf{z}\|_2^2 + \lambda \mathbf{x}^T\mathbf{Wx} \tag{12}$$

where λ is the regularization parameter and depends on ϵ (noise level). Based on [14], we can define $\mathbf{W}$ such that its diagonal elements are

$$W_{ii} = (\eta + \mid \hat{x}_{0,i} \mid)^{-1}$$

where $\hat{x}_{0,i}$ represents the ith component of the estimated solution $\hat{\mathbf{x}}$, which is found by minimizing $(1/2)\mathbf{x}^T\mathbf{x}$ subject to $\mathbf{Ax}=\mathbf{z}$. Experimental results show that choosing η in the range to [0.001, 0.01] is helpful to get the accurate solution. The solution to (12) is

$$\hat{\mathbf{x}} = \left(\mathbf{A}^T\mathbf{A} + \lambda\mathbf{W}\right)^{-1}\mathbf{A}^T\mathbf{z}. \tag{13}$$

The first term in (12) minimizes the residual error, whereas the second term is the regularization factor that encourages sparsity in the successive solutions. In order to reduce the computational cost, we can rewrite (13) as

$$\hat{\mathbf{x}} = \mathbf{W}^{-1}\mathbf{A}^T\left(\mathbf{AW}^{-1}\mathbf{A}^T + \lambda\mathbf{I}\right)^{-1}\mathbf{z}. \tag{14}$$

We choose $\sigma_0 = 4 * \max|\hat{\mathbf{x_0}}|$ as the initial value for σ, then $f_\sigma(x) \approx 1$, which makes the $F_\sigma(\mathbf{x})$ less likely to get trapped into the local maxima, and also accelerates the convergence speed. To summarize, the modified smoothed L_0 norm algorithm is depicted in Table I.

IV. Real Data Processing

In order to demonstrate the superiority of MSL_0-based imaging approach, the experimental results of the SL_0 norm, L_1 norm, and weighted L_1 norm (WL_1) algorithms are presented as well. We use a set of real data of Yak-42 plane and present the experimental results in this section. The parameters of radar are listed in Table II. In the following experiments, 128 pulses within a dwell time of [-0.64, 0.64] s are used. To illustrate the superiority of the algorithms, we add white

TABLE I
Modified Smoothed L_0 Norm Algorithm

Step 1: Initialization $\hat{\mathbf{x_0}} = \mathbf{W}^{-1}\mathbf{A}^T(\mathbf{AW}^{-1}\mathbf{A}^T + \lambda\mathbf{I})^{-1}\mathbf{z}$;
set $\sigma_{\min} \in [0.01, 0.001]$, which depends on the noise power;
set the decreased factor as $\xi = 0.5$ and the step-size parameter as $\mu = 2$.

Step 2: Set $\sigma_0 = 4 * \max|\hat{\mathbf{x_0}}|$ and maximize the function F_σ:
While $\sigma > \sigma_{min}$
  For $l = [1, \cdots, L]$
    $\delta = [x_1 e^{-\frac{x_1^2}{2\sigma^2}}, \cdots, x_n e^{-\frac{x_n^2}{2\sigma^2}}]$
    $\mathbf{x} = \mathbf{x} - \mu\delta$
    If $\|\mathbf{Ax}-\mathbf{z}\|_2 \geq \epsilon$
      $\mathbf{x} = \mathbf{x} - \mathbf{A}^T(\mathbf{AA}^T)^{-1}(\mathbf{Ax}-\mathbf{z})$
    end
  end
  $\sigma = \xi * \sigma$
end

Step 3: Output the final solution: $\hat{\mathbf{x}} = \mathbf{x}$.

TABLE II
Radar System Parameters

Radar Parameters	Values
Bandwidth	400MHz
Carrier Frequency	10GHz
Pulse Repetition Frequency	100Hz
Range Resolution	0.375m

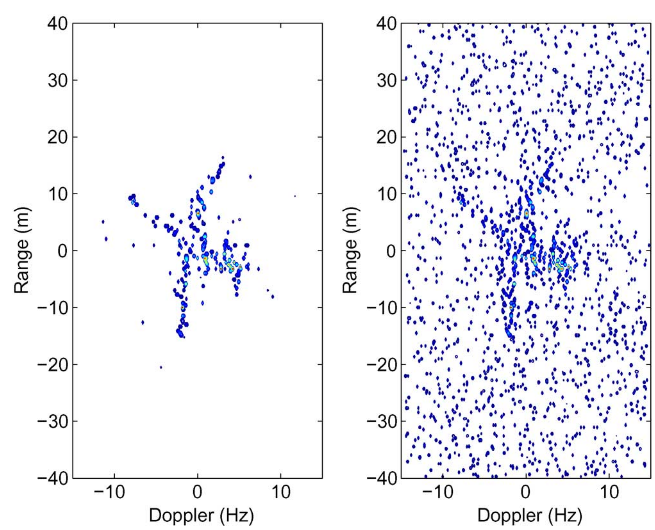

Fig. 1. Images under SNR of 5 dB with constant pulse number, i.e., 32.

Gaussian noise to the real measured data to obtain different signal-to-noise ratios (SNRs) and use different pulse numbers (i.e. 64, 32, and 8 pulses) in our experiments. Furthermore, the experimental results show that choosing λ in the range to [0.1, 2] is helpful to get accurate solution at different SNRs.

From Fig. 1, we can observe that the MSL_0-based approach has a better performance than the SL_0-based algorithm under the same conditions. In particular, the MSL_0-based approach is able to recover the image with much less artificial points and extracts more scattering centers of the plane.

Figs. 2 and 3 indicate that the image obtained by the MSL_0 norm algorithm is more unambiguous than the SL_0 [9], L_1 norm [13], and weighted L_1 norm [13] algorithms.

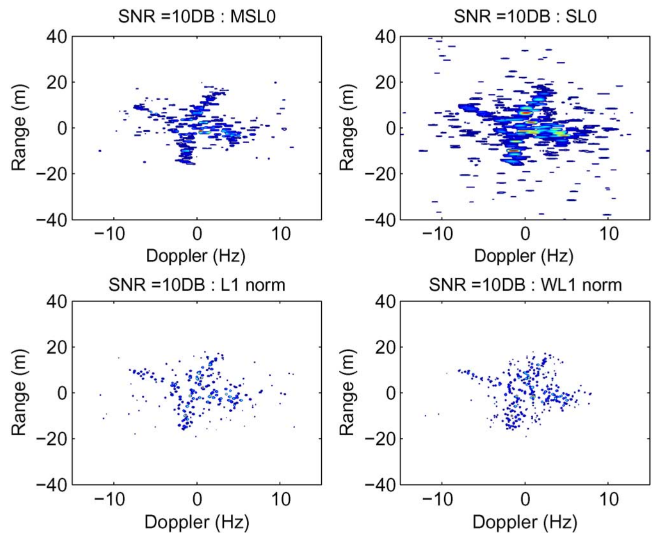

Fig. 2. Images under SNR of 10 dB with constant pulse number, i.e., 8.

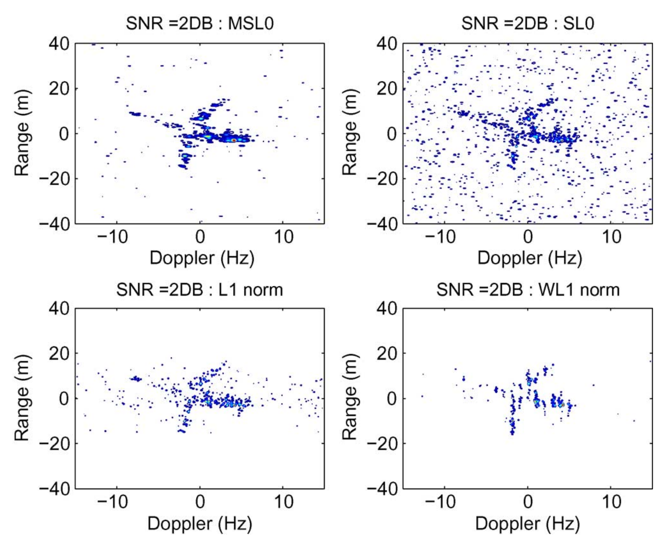

Fig. 3. Images under SNR of 2 dB with constant pulse number, i.e., 64.

Let us now evaluate the computational complexity of the imaging algorithms. In our experiments, we use the CPU time as the processing time that was measured on an Intel Processor 2.60 GHz with 4 GB RAM. All simulations are performed in the MATLAB 7.0 environment. Although it is not an exact measure, the processing time gives a rough estimation of the complexity, enabling us to compare the MSL_0 norm algorithm with the other three algorithms. We have repeated 1000 times for each algorithm, and the values of the processing time are obtained by averaging the simulations. Table III implies that the MSL_0 norm algorithm is faster than the SL_0 [9], L_1 norm [13], and weighted L_1 norm [13] algorithms. As pointed out in [9], the complexity relationship between SL_0 norm algorithm and L_1 norm algorithm is about two or three orders of magnitude.

TABLE III
PROCESSING TIME FOR IMAGING UNDER SNR OF 2 dB WITH 64 PULSES

Algorithm	Time (sec)
MSL_0 norm	4.2
SL_0 norm	6.4
L_1 norm	108.9
WL_1 norm	115.6

V. CONCLUSION

In this letter, we have devised the modified smoothed L_0 norm algorithm for inverse synthetic aperture radar imaging. The experiments of real data show that our proposal provides better imaging performance and requires much less computational complexity. However, the proposed algorithm cannot adaptively determine the parameters λ, η, and μ, like [9], [14], and [15]. That is to say, they are all empirical values. In our future work, this problem will be tackled in the form of adaptive adjustment.

REFERENCES

[1] D. L. Mensa, *High Resolution Radar Cross-Section Imaging*. Dedham, MA, USA: Artech House, 1981.

[2] Y. H. Zhang and X. K. Zhang, “Moving train imaging by ground-based ka-band radar,” in *Proc. Loughborough Antennas Propag. Conf.*, Loughborough, U.K., Nov. 16–18, 2009, pp. 413–416.

[3] E. Walton and A. Moghaddar, “High resolution imaging of radar targets using narrow band data,” in *Proc. IEEE AP-S Int. Symp.*, Jun. 1991, pp. 1020–1024.

[4] H. R. Jeong, H. T. Kim, and K. T. Kim, “Application of subarray averaging and entropy minimization algorithm to stepped-frequency ISAR autofocus,” *IEEE Trans. Antennas Propag.*, vol. 56, no. 4, pp. 1144–1154, Apr. 2008.

[5] Y. Zhong and X. Chen, “MUSIC imaging and electromagnetic inverse scattering of multiply scattering small anisotropic spheres,” *IEEE Trans. Antennas Propag.*, vol. 55, no. 12, pp. 3542–3549, Dec. 2007.

[6] D. L. Donoho, M. Elad, and V. N. Temlyakov, “Stable recovery of sparse overcomplete representations in the presence of noise,” *IEEE Trans. Inf. Theory*, vol. 52, no. 1, pp. 6–18, Jan. 2006.

[7] S. S. Chen, D. L. Donoho, and M. A. Saunders, “Atomic decomposition by basis pursuit,” *SIAM J. Sci. Comput.*, vol. 43, no. 1, pp. 129–159, Aug. 2006.

[8] J. Dai, D. Zhao, and X. Ji, “A sparse representation method for DOA estimation with unknown mutual coupling,” *IEEE Antennas Wireless Propag. Lett.*, vol. 11, pp. 1210–1213, 2012.

[9] H. Mohimani, M. Babaie-Zadeh, and C. Jutten, “A fast approach for overcomplete sparse decomposition based on smoothed L_0 norm,” *IEEE Trans. Signal Process.*, vol. 57, no. 1, pp. 289–301, Jan. 2009.

[10] E. Candès, J. Romberg, and T. Tao, “Robust uncertainty principles: Exact signal reconstruction from highly incomplete frequency information,” *IEEE Trans. Inf. Theory*, vol. 52, no. 2, pp. 489–509, Feb. 2006.

[11] D. L. Donoho, “Compressed sensing,” *IEEE Trans. Inf. Theory*, vol. 52, no. 4, pp. 5406–5425, Apr. 2006.

[12] E. Candès, “The restricted isometry property and its implications for compressed sensing,” *C. R. l’Academie des Sciences, ser. I*, vol. 364, no. 5, pp. 589–592, May 2008.

[13] L. Zhang, M. D. Xing, and Z. Bao, “Resolution enhancement for inversed synthetic aperture radar imaging under low SNR via improved compressive sensing,” *IEEE Trans. Geosci. Remote Sens.*, vol. 48, no. 10, pp. 3824–3838, Oct. 2010.

[14] Y. Kopsinis, K. Slavakis, and S. Theodoridis, “Online sparse system identification and signal reconstruction using projections onto weighted l_1 balls,” *IEEE Trans. Signal Process.*, vol. 59, no. 3, pp. 905–930, Mar. 2011.

[15] A. Eftekhari, M. Babaie-Zadeh, and C. Jutten, “Robust-SL0 for stable sparse representation in noisy settings,” in *Proc. IEEE Int. Conf. Acoust., Speech, Signal Process.*, Apr. 2009, pp. 3433–3436.